Published in final edited form as:
Neurobiol Dis. 2019 September 05; 132: 104605. doi:10.1016/j.nbd.2019.104605.

Subthalamic nucleus oscillations correlate with vulnerability to freezing of gait in patients with Parkinson's disease

Chiung-Chu Chen[a,b,c,*], **Chien-Hung Yeh**[a,d,e], **Hsiao-Lung Chan**[b,f], **Ya-Ju Chang**[b,g], **Po-Hsun Tu**[c,h], **Chih-Hua Yeh**[c,i], **Chin-Song Lu**[a,b,j], **Petra Fischer**[d,e], **Gerd Tinkhauser**[d,e,k], **Huiling Tan**[#d,e], **Peter Brown**[#d,e]

[a]Division of Movement Disorders, Department of Neurology, Chang Gung Memorial Hospital, Linkou, Taiwan [b]Neuroscience Research Center, Chang Gung Memorial Hospital, Linkou, Taiwan [c]School of Medicine, College of Medicine, Chang Gung University, Taoyuan, Taiwan [d]Medical Research Council Brain Network Dynamics Unit at the University of Oxford, OX1 3TH Oxford, United Kingdom [e]Nuffield Department of Clinical Neurosciences, John Radcliffe Hospital, University of Oxford, OX3 9DU Oxford, United Kingdom [f]Department of Electrical Engineering, College of Engineering, Chang Gung University, Taoyuan, Taiwan [g]School of Physical Therapy and Graduate Institute of Rehabilitation Science, College of Medicine, Healthy Aging Research Center, Chang Gung University, Taoyuan, Taiwan [h]Department of Neurosurgery, Chang Gung Memorial Hospital, Linkou, Taiwan [i]Department of Neuroradiology, Chang Gung Memorial Hospital, Linkou, Taiwan [j]Professor Lu Neurological Clinic, Taoyuan, Taiwan [k]Department of Neurology, Bern University Hospital and University of Bern, Bern, Switzerland

[#] These authors contributed equally to this work.

Abstract

Freezing of gait (FOG) is a disabling clinical phenomenon often found in patients with advanced Parkinson's disease (PD). FOG impairs motor function, causes falls and leads to loss of independence. Whereas dual tasking that distracts patients' attention precipitates FOG, auditory or visual cues ameliorate this phenomenon. The pathophysiology of FOG remains unclear. Previous studies suggest that the basal ganglia are involved in the generation of FOG. Investigation of the modulation of neuronal activities within basal ganglia structures during walking is warranted. To this end, we recorded local field potentials (LFP) from the subthalamic nucleus (STN) while PD patients performed single-task gait (ST) or walked while dual-tasking (DT). An index of FOG (iFOG) derived from trunk accelerometry was used as an objective measure to differentiate FOG-vulnerable gait from normal gait. Two spectral activities recorded from the STN region were associated with vulnerability to freezing. Greater LFP power in the low beta (15–21 Hz) and theta (5–8 Hz) bands were noted during periods of vulnerable gait in both ST and DT states. Whereas the elevation of low beta activities was distributed across STN, the increase in theta activity was focal and found in ventral STN and/or substantia nigra (SNr) in ST. The results demonstrate that

[*]Corresponding author at: Division of Movement Disorders, Department of Neurology, Chang Gung Memorial Hospital, 333, Taoyuan, Taiwan. neurozoe@gmail.com (C.-C. Chen).

Declaration of Competing Interest
The authors declare no competing financial interests.

Europe PMC Funders Author Manuscripts

low beta and theta band oscillations within the STN area occur during gait susceptible to freezing in PD. They also add to the evidence that narrow band ~18 Hz activity may be linked to FOG.

Keywords

Parkinson's disease; FOG; Subthalamic nucleus; Local field potentials (LFPs)

1 Introduction

Freezing of gait (FOG) is a common and disabling motor disturbance in patients with Parkinson's disease (PD). It is defined as “brief, episodes of inability to generate effective forward stepping movement despite the intention to walk” (Bloem et al., 2004; Giladi et al., 2001; Nutt et al., 2011), often occurring during initiation of gait, on turning while walking, passing doorways or approaching destination (Spildooren et al., 2010; Snijders et al., 2010, 2016). At the advanced stage, this clinical phenomenon even occurs during straight walking in open space (Snijders et al., 2010). Several features are often observed during FOG. The feet are not able to leave the ground and patients feel the feet are stiff and “glued on the floor”. Trembling of the legs at a frequency of 3–8 Hz, so called “trembling in place” (Moore et al., 2007), hastening and shuffling gait can also co-occur. FOG often leads to falls and injuries and loss of autonomy in daily life. It remains unclear whether the variability of features reflects the spectrum of a common pathogenesis or arises from different neural networks.

The occurrence of FOG usually depends on situations. It is elicited when patients are passing crowded places, are under stress or are distracted by a second, unrelated task (dual-tasking). In contrast, auditory or visual cues and attention often ameliorate FOG. Due to the fact that cognitive, emotional and environmental factors have a striking influence on the vulnerability to FOG, it can be surprisingly difficult to capture and assess the occurrence of FOG in the laboratory. So far, only limited physiological studies have defined state markers of FOG during walking (Hell et al., 2018; Singh et al., 2013; Snijders et al., 2010).

The therapeutic modulation of FOG is complex (Ferraye et al., 2008a). Freezing often occurs at the nadir of levodopa and is ameliorated during the on medication state (Schaafsma et al., 2003). As the disease progresses, FOG becomes more resistant to L-dopa therapy. Deep brain stimulation (DBS) in the subthalamic nucleus (STN) improves FOG in the off-medication state (Ferraye et al., 2008b), indicating this structure is involved in the pathogenesis of freezing. However, the failure of response to high frequency stimulation of STN in some patients with FOG has contributed to the exploration of other stimulation targets or low frequency stimulation paradigms (Stefani et al., 2007; Plaha and Gill, 2005; Moreau et al., 2008).

The pathophysiology of FOG is unclear. Studies in animals, functional imaging and neurophysiology experiments on patients with PD suggest that the basal ganglia, supplementary motor area (SMA) and midbrain locomotor region (MLR) are responsible for FOG in PD (Lewis and Barker, 2009). It is suggested that the basal ganglia play important roles in effectively switching activity between competing yet complimentary neural

Europe PMC Funders Author Manuscripts

networks (Shine et al., 2013b). The dysfunction of the basal ganglia due to dopamine depletion may result in the disruption of descending control of the midbrain locomotor area and consequently lead to FOG (Hallett, 2008).

In this study, we recorded local field potentials from the area of the STN of Parkinsonian patients during walking. Oscillatory activity in the STN area was assessed during gait with and without a second task, hereafter termed single-task gait (ST) and dual-task gait (DT).

2 Materials and methods

2.1 Patients and surgery

The patients (n = 15, mean age 61.8 ± 5.0 years, range 52–69, 7 male) participated with informed consent and the permission of the local ethics committee of Chang Gung Memorial Hospital. All were advanced idiopathic PD with motor fluctuation and/or dyskinesia. The mean disease duration was 14.9 ± 4.8 years. Preoperative assessments included the motor experience of daily living (part 2), motor examination (part 3) and complications (part 4) of the Unified Parkinson's Disease Rating Scale (UPDRS). These were used to differentiate the tremor-dominant (TD) subtype from that with postural instability and gait difficulty (PIGD) (Jankovic et al., 1990; Jankovic, 2008). Global cognition was assessed with the Mini-Mental State Examination (MMSE) and severity of depression was assessed using Beck Depression Inventory (BDI) (Table 1). Off medication assessments were taken after overnight withdrawal of dopaminergic medication. Three cases presented here were reported previously (Fischer et al., 2018).

Implantation of bilateral STN DBS electrodes was performed sequentially in the same operative session under local anesthesia in all patients. The DBS electrode used was model 3389 (Medtronic Neurological Division, Minneapolis) with four platinum-iridium cylindrical surfaces (1.27 mm diameter and 1.5 mm length) and a center-to center separation of 2 mm. Contact 0 was the lowermost and contact 3 was the uppermost.

Patients underwent whole brain magnetic resonance images (MRI) before operation. Whole brain axial T1W1, T2W1 3D MR images were obtained for evaluation of target nucleus and trajectory planning. Direct targeting was made through superimposing MRI on stereotactic computerized tomography (CT) to identify the location of STN region. The planning of targeting was further confirmed by using indirect stereotactic CT to overcome possible image distortions. The intended coordinates of STN were 12 mm lateral from the midline, 3 mm behind the midcommissural point, and 4–5 mm below the anterior commissural-posterior commissural line. Targeting was facilitated by microelectrode recordings (MER). The most caudal contact was placed in the substantia nigra (SNr) when clear SNr neuronal activities were identified. Otherwise, this contact was placed below the lower border of STN. As the MER detected STN span was 5.2 ± 1.3 mm in this patient cohort, the middle two contacts likely lay in STN and the rostral contact above the upper border of STN.

Soon after bilateral STN electrodes were implanted, twelve patients underwent whole brain MRI scans. The whole brain 3D T1W1 and T2W1 scans were acquired in the axial plane and reconstructed in oblique-sagittal and oblique-coronal fashion along the electrodes. For

another three patients, the STN was only identified from high-resolution T2-weighted MRI (patient 5, 7, 8). The MR images were reviewed on a stereotactic workstation to confirm the locations of the DBS electrodes and to exclude potential surgery-related complications.

Post-operative contact localization was performed by using the MATLAB-based software (Lead-DBS) (Horn and Kühn, 2015; Horn et al., 2019) to reconstruct the DBS electrode placement based on pre and post-operative MR images in 12 patients with whom post-operative whole brain 3D MRI were available. Localization of contacts was therefore obtained from 24 DBS electrodes. All pre and post-operative sequences were co-registered using SPM 12 toolbox. Subsequent linear co-registration between patient and template space, and nonlinear brain shifts were performed following the approach introduced by Schonecker et al. Co-registration and brain shift correction results were then checked manually using built-in tools. Electrode location was defined by a built-in manual click-and-point tool. The quadripolar DBS electrodes comprising four metallic contacts at equidistant intervals generate susceptibility artifacts on MRI. The centers of the artifacts show as hypointense and represent the centers of the electrode contacts. Final 3D rendering of STN leads was demonstrated in synopsis with key structures defined by the Human Motor Thalamus atlas (Fig. 1) (Jakab et al., 2012).

2.2 Paradigm

Patients were assessed “off-medication”, after overnight withdrawal of dopaminergic medication. Experiments took place 3–5 days after DBS electrodes were implanted, in the interval between macroelectrode implantation and the subsequent connection to a subcutaneously placed stimulating device (Activa, Medtronic, USA). We recorded two conditions: single-task gait (ST) and dual-task gait (DT). Patients were asked to walk straight on a GAITRite carpet (CIR system, Clifton, New Jersey, USA) at their own preferred speed during either ST or DT. Walking was uncued. In DT, three different cognitive tasks were projected on a screen in front of the patients while walking. The three types of tasks were serial subtraction, color Stroop and a spatial memory task. In the serial subtraction task, the subject read the number projected on the screen and subtracted three from the number consecutively, five times. In the Stroop task, patients were instructed to name the color of the projected word which was incongruent with the color. To challenge spatial memory, patients were required to remember the spatial sequence of three yellow blocks in a 3 by 3 grid. They would then read out the numbers that corresponded to the locations where the yellow blocks appeared after a grid with numbers in all 9 blocks was shown. Patients were encouraged to complete two trials for each condition and task (two trials for ST and six for DT). The DT was thought to maximize the chances of FOG (Kelly et al., 2012). The occurrence of freezing in these patients at the time of test was confirmed by a movement disorders specialist (C. C. C.).

2.3 Recordings

Local field potentials (LFPs) were recorded in monopolar configuration from four contacts of each electrode. LFPs were sampled at 2048 Hz and amplified. A triaxial accelerometer was taped over the spinous processes at the upper lumbar level to record trunk acceleration. Patients carried a portable battery-charged amplifier (TMSI international) in a backpack and

the data were recorded on a laptop (software written by Pogosyan A) via a long fibre-optic cable.

2.4 Data analysis

All data were converted to Spike 2 (Cambridge electronic design) before further analysis using custom-written MATLAB scripts.

Accelerometry (ACC) data were down-sampled to 100 Hz and the index of freezing of gait (iFOG) was estimated off-line. The accelerometer axis with the largest deflections consistent with gait (usually in the anterior-posterior plane) was used for analysis (Moore et al., 2008). The iFOG measure is based on the observation that FOG entails an increase in high-frequency (3–8 Hz) leg activity in the relative absence of lower-frequency (< 3 Hz) locomotion, so that the ratio between these two bands serves as a marker of FOG. The estimation of iFOG and its dependence on different experimental parameters has been previously described in detail (Moore et al., 2013). The size of the sampling window for each iFOG estimate was three seconds (Moore et al., 2008).

Common average LFP data were re-referenced offline to obtain more spatially focal bipolar signals by subtracting the data from neighboring electrode contacts. Bipolar LFP data were down-sampled to 1000 Hz and high-pass filtered (1 Hz cut-off, Butterworth filter, filter order = 6, passed forwards and backwards) before further analyses using the fieldtrip-function ft_freqanalysis (Oostenveld et al., 2011).

The continuous Morlet wavelet transform was applied to achieve time-frequency decomposition. The wavelets were set to span 6 cycles. The resulting time-frequency decomposition was down-sampled to 200 Hz. LFP power was assessed by 1-Hz frequency bins, spanning from 5 to 50 Hz. Relative power was obtained for each subject and frequency in each window by normalizing the absolute power by its average across time for each channel: (power − average power) / average power ∗ 100. To compare the power spectrum across different periods of interest (i.e., normal and vulnerable gait periods, or ST and DT), we separately normalized each period by the average of the entire LFP recording.

2.5 Statistics

Spearman's correlation coefficients were computed between the UPDRS II item 14 score and iFOG. The analyzed duration of walking was 41.0 ± 8.2 s (n = 13) and 120.2 ± 27.6 s (n = 13) for ST and DT, respectively. Results are reported as mean ± standard error and two-tailed p values < .05 were considered statistically significant (α = 0.05 for all hypothesis testing). Repeated measures ANOVAs were performed as described in the results and Scheffe's procedure was used for post-hoc comparisons.

3 Results

3.1 Post-operative contact localization

Reconstruction of contact site was possible in 24 DBS electrodes. However, due to factors such as electrode artefact and variability of structures, these reconstructions should be considered as supportive evidence rather than proof of targeting. Among the 24 electrodes

all had at least one contact within STN on reconstruction. Fifteen lower-most contact pairs (01) involved contacts below STN with 10 contacts within SNr. All but two of the middle contact pairs (12) involved one ($n = 9$) or both ($n = 13$) contacts in STN. Of the dorsal contact pairs (23), one ($n = 8$) or both contacts ($n = 5$) were thought to lie above STN. Both contacts were within STN in 9 contact pairs. In two DBS electrodes, the uppermost contact pairs bridged the lower border of the STN (both sides in patient 15). The precise distribution of different contacts is summarized in Fig. 1B, while Fig. 1A illustrates data from patient 10.

3.2 Kinematic parameters of gait

Gait parameters were extracted and computed after collecting the walking sequences from the GAITRite system (Table 2). All patients completed both ST and DT except 4 (patients 1, 5, 11 and 15). The duration of FOG ranged from 3 to 19 s (6.8 ± 4.3 s) in the three cases (patients 6, 11 and 14) demonstrating FOG.

The face-validity of iFOG estimates was supported by its higher value during dual tasking when FOG is more likely (paired *t*-test, $p = .0262$) (Fig. 2). In addition, the occurrence of FOG was confirmed by a movement disorders specialist in three subjects (patients 6, 11 and 14) on the day of assessment. These represented the patients with the highest, second highest and seventh highest iFOG scores. Fig. 3 shows an example of gait period categorization using ACC power and iFOG. Total ACC power was used to differentiate standing from walking, whereas iFOG was used to differentiate normal from gait periods with an increased vulnerability to FOG.

3.3 Differences between single-task gait and dual tasking

Fig. 4 contrasts relative power changes between ST and DT in each bipolar channel (i.e., C01, C12, and C23) across the group. Of note the relative power here was normalized by the averaged power of all walking periods, i.e., ST plus DT, in each frequency bin for each bipolar channel in each subject, before averaging. There was significantly higher relative power in DT than in ST centered around 18 Hz, in the beta band. This was most prominent in C12. For further quantitative analysis, we averaged beta power around the peak in modulation from 15 to 21 Hz during ST and DT and subtracted the two, for each hemisphere. An ANOVA with hemisphere (two levels, left and right), electrode contact (three levels, C01, C12 and C23), and condition (two levels, ST and DT) as factors revealed only a main effect of condition ($p = .0002$) (Table 3). DT increased relative beta power by 17.7 ± 9.6% comparing with ST.

3.4 Differences between low and high iFOG gait periods

Although freezing is more likely and the iFOG greater during DT the above analysis cannot distinguish between a difference in spectral activity that relates to the propensity for freezing from that due to the dual tasking per se. We therefore sought explicit differences in relative power between normal and vulnerable gait during either ST or during DT (Fig. 5A and B, respectively). LFP power was classified as occurring during normal or vulnerable gait by median-splitting the data according to the iFOG in each patient and gait condition. The results showed that beta power was higher during vulnerable (higher iFOG) compared to more normal (lower iFOG) gait in both ST and DT. The effect was present across all

contacts, but greatest at contact 12, where it was also significant. This analysis also revealed greater theta (5-8 Hz) power during vulnerable gait compared to normal ST at contact 01, and during vulnerable DT gait compared to normal DT gait across all contacts.

Quantitative analysis was performed by a series of ANOVAs. These were performed separately for ST and DT as the median split according to iFOG within each condition would not identify equivalent periods of vulnerability to FOG. Specifically, the upper subgroup in a median split of DT data would identify LFPs associated with higher iFOG values than in the upper subgroup in a median split of ST data. An ANOVA of mean relative 15–21 Hz power in the ST condition with hemisphere (two levels, left and right), electrode contact (three levels, C01, C12 and C23), and FOG vulnerability (two levels, vulnerable and normal gait) as factors only revealed a significant effect of FOG vulnerability ($p = .0374$) (Table 4). The relative power increase over 15–21 Hz averaged across all three contacts was 7.3 ± 8.0% in this condition. An additional ANOVA of mean relative theta power in the ST condition with the same factors revealed a significant interaction between FOG vulnerability and contact pairs ($p = .0025$) (Table 5). This was further explored by separate ANOVAs for each contact pair with factors condition and hemisphere (Table 6). The results show that theta power was only different between periods of low and high iFOG in the theta band at contact pair 01 ($p = .0009$). Here, theta activity increased to 31.4 ± 12.5% in the elevated FOG vulnerability data.

An ANOVA of mean relative 15–21 Hz power in the DT gait condition with hemisphere (two levels, left and right), electrode contact (three levels, C01, C12 and C23), and FOG vulnerability (two levels, high and low median split iFOG) as factors only revealed a significant effect of FOG vulnerability ($p = .0013$) (Table 7). The relative power increase over 15–21 Hz averaged across all three contacts was 16.7 ± 7.7% in this condition. An additional ANOVA of mean relative theta power in the DT gait condition with the same factors as above also revealed only a significant effect of FOG vulnerability ($p < .0001$) (Table 8). The relative power increase over 5–8 Hz averaged across all three contacts was 32.4 ± 6.9% in this condition.

Finally, to contrast the spectral changes in the two key bands during periods of relatively increased iFOG we normalized power in the ST and DT gait conditions by the averaged power across ST and DT at each frequency so that LFP changes were comparable. The relative spectral change in periods of elevated iFOG during ST and DT were not significantly different (Table 9).

4 Discussion

In patients with Parkinson's disease, we found that low frequency beta and theta activities in the STN area are modulated during walking. Greater increase of LFP power in both frequency bands was seen when walking was more vulnerable and susceptible to freezing. Whereas the change in low beta power was distributed across all contacts, the modulation of theta band activity was focal and limited to the lower-most contact pair. We have thus identified two spectral correlates of an elevated vulnerability to freezing.

A methodological challenge in the current study is that we chose to use the iFOG as an objective measure to reflect the spectrum of vulnerability to FOG. It should be stressed that we did not use the iFOG to identify freezing episodes as these only occurred in three patients during the gait tasks. Instead we used it to provide an indirect measure of the variation in the susceptibility to freezing during task performance. The use is presumptive, but did serve to identify some state markers, particularly elevated theta and low beta power in high iFOG states. Moreover, while electrophysiological modulation may have been even more marked and relevant during actual freezing events, the absence of overt freezing paradoxically serves to rule out the beta and theta band change being consequent upon afferent feedback related to freezing. The state-dependent changes in oscillatory activity in the subthalamic area should also be distinguished from step-aligned modulation of LFP activity in the upper beta frequency band (Fischer et al., 2018), or over a broader range of frequencies (Hell et al., 2018) reported in the STN. It should also be noted that one patient, case 2, historically had levodopa unresponsive FOG, which may possibly have a different pathophysiology to levodopa responsive FOG.

Despite demonstrating the spectral associations we do not provide evidence that theta and low beta activities are causally important in FOG. Excessive synchronized neuronal activities in the beta frequency range (13–35 Hz) in parkinsonian STN at rest and the relative failure of their suppression during action have been repeatedly linked to brady-kinesia and rigidity (Kühn et al., 2004). Abnormal beta oscillations have been found in patients with FOG during rest (Toledo et al., 2014), walking (Singh et al., 2013) and bicycling (Storzer et al., 2017). Increased high frequency beta activity was noted in patients with levo-dopa-responsive FOG at rest when compared with non-freezers (Toledo et al., 2014). In contrast to this last observation, oscillatory activity specifically in the low beta band (12–22 Hz) was noted in freezers while broadband beta activity reduced during movement in non-freezers (Singh et al., 2013; Storzer et al., 2017). More specifically, a characteristic ~18 Hz activity in the STN was found exclusively in freezers (Storzer et al., 2017). This is in line with our findings that a narrow band elevation of STN LFP activity at ~18 Hz was predominant during dual-task walking when FOG is more readily triggered (Spildooren et al., 2010).

These findings fit with the proposal that the nature of low beta oscillations is antikinetic (Hammond et al., 2007). In support of this, direct low frequency stimulation of STN at 20 Hz impairs motor performance in PD (Chen et al., 2007; Eusebio et al., 2008; Timmermann and Florin, 2012). The deleterious effect is even more profound when movement of proximal muscles is assessed (Chen et al., 2011). These observations raise the possibility that the excessive synchronization in the low beta range may be mechanistically linked to freezing.

Nevertheless, the hypothesis that low beta activity in the STN may be causal in FOG remains speculative, and other interpretations exist. The PPN comprises part of the so-called MLR in the brain stem and is the final output of the cortico-subcortical loops that regulate gait initiation and adaptation (Garcia-Rill et al., 2015). More recent studies have suggested that low frequency stimulation (40–60 Hz) effectively activates the PPN, whereas high frequency stimulation (> 80 Hz) inactivates the same structure (Garcia-Rill et al., 2019).

PPN stimulation can reduce FOG in some patients (Moro et al., 2010; Thevathasan et al., 2011). In animal models, rostral PPN neurons are strongly interconnected with the basal ganglia, including the STN and globus pallidus interna (Garcia-Rill et al., 2019). Cortical regions, such as supplementary motor area (SMA), may also be involved (Shine et al., 2013a; Snijders et al., 2016).

Surprisingly, the elevation of low beta power during episodes of increased vulnerability to freezing was not focal, but detected across all bipolar contacts. Several factors may have contributed to a lack of focality, including the limited spatial resolution of bipolar electrode contacts, the presence of a temporary stun effect and minor variation in physiology, anatomy and surgical targeting among patients.

What is the relevance of the increase of theta activity when vulnerability to freezing is elevated? The increase did not simply arise due to the attentional demands of dual tasking as it was not elevated in this condition when episodes of higher iFOG were not selected. The functional role of theta may be related to processing of conflict and cognitive interference (Shine et al., 2013a,b, 2014). In line with this, theta oscillations increase at the cortical level during the transition between normal walking and freezing. The increase in theta activity seen in the present study may therefore reflect increased cognitive monitoring necessary when mechanisms supporting gait are weakened and the subject is made more vulnerable to FOG. This occurs during DT but may also occur, at times, in ST, which in our paradigm also included turning to return along the gait path.

Alternatively, it is possible that the elevation of theta activity in the vulnerable gait state might have been due to movement artifacts. Previous studies have shown that one of the important features of FOG in PD is the increase of 3–8 Hz oscillations, so called “trembling in place”. Therefore, the increase in theta band power may be due to mechanical transmission to the recording contacts. However, this seems unlikely as our LFP recordings were bipolar, so that any common signal across contacts would have been subtracted out. Furthermore, one wouldn't expect the elevation of theta activity to be focal and consistently limited to the lowermost contact pair in ST if the modulation arose through movement-related artefact. Given that contact 0 was the intended to be placed in the SNr, then contact 01 was likely to be picking up activity from the SNr or associative areas of the STN. These findings are supported by previous reports that PPN has direct reciprocal connections to STN and SNr (Reese et al., 1995). At a systems level, it has been proposed that the “cross-talk” between motor, cognitive and limbic circuits may overload information processing capacity in the striatum in PD, and lead to synchronized activities in the output structures of the basal ganglia, including the GPi and SNr. This would result in over-inhibition of the PPN and consequently lead to freezing (Ehgoetz Martens et al., 2018).

These results also have clinical implications. The link between vulnerable gait and narrow band beta and theta oscillations in the STN region raises the possibility that patients with FOG may potentially benefit from adaptive DBS whereby on-demand stimulation might only be delivered when the state-related oscillatory pattern exceeds a certain threshold. Nevertheless, this remains speculative and whether the present findings can be translated

into favorable therapeutic interventions for FOG remains to be shown in further clinical trials.

5 Conclusion

This study adds to the evidence that there is a narrow band elevation of STN LFP activity at around 18 Hz in patients during periods of gait with increased vulnerability to FOG, further linking this activity to FOG. In addition, we identified elevation of theta activity in periods of increased vulnerability to FOG, with this being confined to the most ventral electrode contact pair during single-task gait. Further work is necessary to establish whether these biomarkers are also increased during actual freezing of gait.

Acknowledgements

This work was supported by Ministry of Science and Technology, Taiwan (MOST 102-2923-B-182-001-MY3), National Research Institute, Taiwan (NHRI-EX-104-7-10413NC) and Chang Gung Memorial Hospital (CMRPG3B1431 and 1432). C.-H.Y. was funded by Postdoctoral Research Abroad Program sponsored by Ministry of Science and Technology in Taiwan (106-2917-I-564-027) and by the Rosetrees Trust. P.B. and H.T. were supported by the Medical Research Council (MC_UU_12024/1). P.B. was further funded by the National Institute of Health Research Oxford Biomedical Research Centre. H.T. was additionally funded by Medical Research Council (MR/P012272/1). We thank Prof. Shih-Tseng Lee for operating on patients. We thank all patients for their collaboration and contribution for the data recordings.

References

Bloem BR, Hausdorff JM, Visser JE, Giladi N. Falls and freezing of gait in Parkinson's disease: a review of two interconnected, episodic phenomena. Mov Disord. 2004; 19:871–884. [PubMed: 15300651]

Chen CC, Litvak V, Gilbertson T, Kühn A, Lu CS, Lee ST, Tsai CH, Tisch S, Limousin P, Hariz M, Brown P. Excessive synchronization of basal ganglia neurons at 20 Hz slows movement in Parkinson's disease. Exp Neurol. 2007; 205:214–221. [PubMed: 17335810]

Chen CC, Lin WY, Chan HL, Hsu YT, Tu PH, Lee ST, Chiou SM, Tsai CH, Lu CS, Brown P. Stimulation of the subthalamic region at 20 Hz slows the development of grip force in Parkinson's disease. Exp Neurol. 2011; 231:91–96. [PubMed: 21683700]

Ehgoetz Martens KA, Hall JM, Georgiades MJ, Gilat M, Walton CC, Matar E, Lewis SJG, Shine JM. The functional network signature of heterogeneity in freezing of gait. Brain. 2018; 141:1145–1160. [PubMed: 29444207]

Eusebio A, Chen CC, Lu CS, Lee ST, Tsai CH, Limousin P, Hariz M, Brown P. Effects of low-frequency stimulation of the subthalamic nucleus on movement in Parkinson's disease. Exp Neurol. 2008; 209:125–130. [PubMed: 17950279]

Ferraye MU, Debû B, Pollak P. Deep brain stimulation effect on freezing of gait. Mov Disord. 2008a; 23:S489–S494. [PubMed: 18668617]

Ferraye MU, Debû B, Fraix V, Xie-Brustolin J, Chabardès S, Krack P, Benabid AL, Pollak P. Effects of subthalamic nucleus stimulation and levodopa on freezing of gait in Parkinson disease. Neurology. 2008b; 70:1431–1437. [PubMed: 18413568]

Fischer P, Chen CC, Chang YJ, Yeh CH, Pogosyan A, Herz DM, Cheeran B, Green AL, Aziz TZ, Hyam J, Little S, et al. Alternating modulation of subthalamic nucleus beta oscillations during stepping. J Neurosci. 2018; 38:5111–5121. [PubMed: 29760182]

Garcia-Rill E, Luster B, D'Onofrio S, Mahaffey S. Arousal, motor control, and Parkinson's disease. Transl Neurosci. 2015; 6:198–207. [PubMed: 27747095]

Garcia-Rill E, Tackett AJ, Byrum SD, Lan RS, Mackintosh SG, Hyde JR, Bisagno V, Urbano FJ. Local and relayed effects of deep brain stimulation of the pedunculopotine nucleus. Brain Sci. 2019; 9:1–15.

Europe PMC Funders Author Manuscripts

Giladi N, Treves TA, Simon ES, Shabtai H, Orlov Y, Kandinov B, Paleacu D, Korczyn AD. Freezing of gait in patients with advanced Parkinson's disease. J Neural Transm. 2001; 108:53–61. [PubMed: 11261746]

Hallett M. The intrinsic and extrinsic aspects of freezing of gait. Mov Disord. 2008; 23:S439–S443. [PubMed: 18668625]

Hammond C, Bergman H, Brown P. Pathological synchronization in Parkinson's disease: networks, models and treatments. Trends Neurosci. 2007; 30:357–364. [PubMed: 17532060]

Hell F, Plate A, Mehrkens JH, Bötzel K. Subthalamic oscillatory activity and connectivity during gait in Parkinson's disease. NeuroImage: Clinical. 2018; 19:396–405. [PubMed: 30035024]

Horn A, Kühn AA. Lead-DBS: a toolbox for deep brain stimulation electrode localizations and visualizations. Neuroimage. 2015; 107:127–135. [PubMed: 25498389]

Horn A, Li N, Dembek TA, Kappel A, Boulay C, Ewert S, Tietze A, Husch A, Perera T, Neumann WJ, Reisert M, et al. Lead-DBS v2: towards a comprehensive pipeline for deep brain stimulation imaging. NeuroImage. 2019; 184:293–316. [PubMed: 30179717]

Jakab A, Blanc R, Berenyi E, Székely G. Generation of individualized thalamus target maps by using statistical shape models and thalamocortical tractography. Am J Neuroradiol. 2012; 33:2110–2116. [PubMed: 22700756]

Jankovic J. Parkinson's disease: clinical features and diagnosis. J Neurol Neurosurg Psychiatry. 2008; 79:368–376. [PubMed: 18344392]

Jankovic J, McDermott M, Carter J, Gauthier S, Goetz C, Golbe L, Huber S, Koller W, Olanow C, Shoulson I, Stern M, et al. Variable expression of Parkinson's disease A base-line analysis of the DATATOP cohort. Neurology. 1990; 40:1529–1534. [PubMed: 2215943]

Kelly VE, Eusterbrock AJ, Shumway-Cook A. A review of dual-task walking deficits in people with Parkinson's disease: motor and cognitive contributions, mechanisms, and clinical implications. Parkinsons Dis. 2012; doi: 10.1155/2012/918719

Kühn AA, Williams D, Kupsch A, Limousin P, Hariz M, Schneider GH, Yarrow K, Brown P. Event-related beta desynchronization in human subthalamic nucleus correlates with motor performance. Brain. 2004; 127:735–746. [PubMed: 14960502]

Lewis SJ, Barker RA. A pathophysiological model of freezing of gait in Parkinson's disease. Parkinsonism Relat Disord. 2009; 15:333–338. [PubMed: 18930430]

Moore O, Peretz C, Giladi N. Freezing of gait affects quality of life of peoples with Parkinson's disease beyond its relationships with mobility and gait. Mov Disord. 2007; 22:2192–2195. [PubMed: 17712856]

Moore ST, MacDougall HG, Ondo WG. Ambulatory monitoring of freezing of gait in Parkinson's disease. J Neurosci Methods. 2008; 167:340–348. [PubMed: 17928063]

Moore ST, Yungher DA, Morris TR, Dilda V, MacDougall HG, Shine JM, Naismith SL, Lewis SJG. Autonomous identification of freezing of gait in Parkinson's disease from lower-body segmental accelerometry. J Neuroeng Rehabil. 2013; 10:19. [PubMed: 23405951]

Moreau C, Defebvre L, Destée A, Bleuse S, Clement F, Blatt JL, Krystkowiak P, Devos D. STN-DBS frequency effects on freezing of gait in advanced Parkinson disease. Neurology. 2008; 71:80–84. [PubMed: 18420482]

Moro E, Hamani C, Poon YY, Al-Khairallah T, Dostrovsky JO, Hutchison WD, Lozano AM. Unilateral pedunculopontine stimulation improves falls in Parkinson's disease. Brain. 2010; 133:215–224. [PubMed: 19846583]

Nutt JG, Bloem BR, Giladi N, Hallett M, Horak FB, Nieuwboer A. Freezing of gait: moving forward on a mysterious clinical phenomenon. Lancet Neurol. 2011; 10:734–744. [PubMed: 21777828]

Oostenveld R, Fries P, Maris E, Schoffelen JM. FieldTrip: open source software for advanced analysis of MEG, EEG, and invasive electrophysiological data. Comput Intell Neurosci. 2011; 2011

Plaha P, Gill SS. Bilateral deep brain stimulation of the pedunculopontine nucleus for Parkinson's disease. Neuroreport. 2005; 16:1883–1887. [PubMed: 16272872]

Reese NB, Garcia-Rill E, Skinner RD. The pedunculopontine nucleus-auditory input, arousal and pathophysiology. Prog Neurobiol. 1995; 47:105–133. [PubMed: 8711130]

Schaafsma J, Balash Y, Gurevich T, Bartels A, Hausdorff JM, Giladi N. Characterization of freezing of gait subtypes and the response of each to levodopa in Parkinson's disease. Eur J Neurol. 2003; 10:391–398. [PubMed: 12823491]

Shine JM, Matar E, Ward PB, Bolitho SJ, Gilat M, Pearson M, Naismith SL, Lewis SJ. Exploring the cortical and subcortical functional magnetic resonance imaging changes associated with freezing in Parkinson's disease. Brain. 2013a; 136:1204–1215. [PubMed: 23485851]

Shine JM, Matar E, Ward PB, Frank MJ, Moustafa AA, Pearson M, Naismith SL, Lewis SJ. Freezing of gait in Parkinson's disease is associated with functional decoupling between the cognitive control network and the basal ganglia. Brain. 2013b; 136:3671–3681. [PubMed: 24142148]

Shine J, Handojoseno A, Nguyen T, Tran Y, Naismith S, Nguyen H, Lewis S. Abnormal patterns of theta frequency oscillations during the temporal evolution of freezing of gait in Parkinson's disease. Clin Neurophysiol. 2014; 125:569–576. [PubMed: 24099920]

Singh A, Plate A, Kammermeier S, Mehrkens JH, Ilmberger J, Bötzel K. Freezing of gait-related oscillatory activity in the human subthalamic nucleus. Basal Ganglia. 2013; 3:25–32.

Snijders AH, Leunissen I, Bakker M, Overeem S, Helmich RC, Bloem BR, Toni I. Gait-related cerebral alterations in patients with Parkinson's disease with freezing of gait. Brain. 2010; 134:59–72. [PubMed: 21126990]

Snijders AH, Takakusaki K, Debu B, Lozano AM, Krishna V, Fasano A, Aziz TZ, Papa SM, Factor SA, Hallett M. Physiology of freezing of gait. Ann Neurol. 2016; 80:644–659. [PubMed: 27649270]

Spildooren J, Vercruysse S, Desloovere K, Vandenberghe W, Kerckhofs E, Nieuwboer A. Freezing of gait in Parkinson's disease: the impact of dual-tasking and turning. Mov Disord. 2010; 25:2563–2570. [PubMed: 20632376]

Stefani A, Lozano AM, Peppe A, Stanzione P, Galati S, Tropepi D, Pierantozzi M, Brusa L, Scarnati E, Mazzone P. Bilateral deep brain stimulation of the pedunculopontine and subthalamic nuclei in severe Parkinson's disease. Brain. 2007; 130:1596–1607. [PubMed: 17251240]

Storzer L, Butz M, Hirschmann J, Abbasi O, Gratkowski M, Saupe D, Vesper J, Dalal SS, Schnitzler A. Bicycling suppresses abnormal beta synchrony in the Parkinsonian basal ganglia. Ann Neurol. 2017; 82:592–601. [PubMed: 28892573]

Thevathasan W, Pogosyan A, Hyam JA, et al. A block to pre-prepared movement in gait freezing, relieved by pedunculopontine nucleus stimulation. Brain. 2011; 134:2085–2095. [PubMed: 21705424]

Timmermann L, Florin E. Parkinson's disease and pathological oscillatory activity: is the beta band the bad guy? —new lessons learned from low-frequency deep brain stimulation. Exp Neurol. 2012; 233:123–125. [PubMed: 22075181]

Toledo JB, López-Azcárate J, Garcia-Garcia D, Guridi J, Valencia M, Artieda J, Obeso J, Alegre M, Rodriguez-Oroz M. High beta activity in the sub-thalamic nucleus and freezing of gait in Parkinson's disease. Neurobiol Dis. 2014; 64:60–65. [PubMed: 24361601]

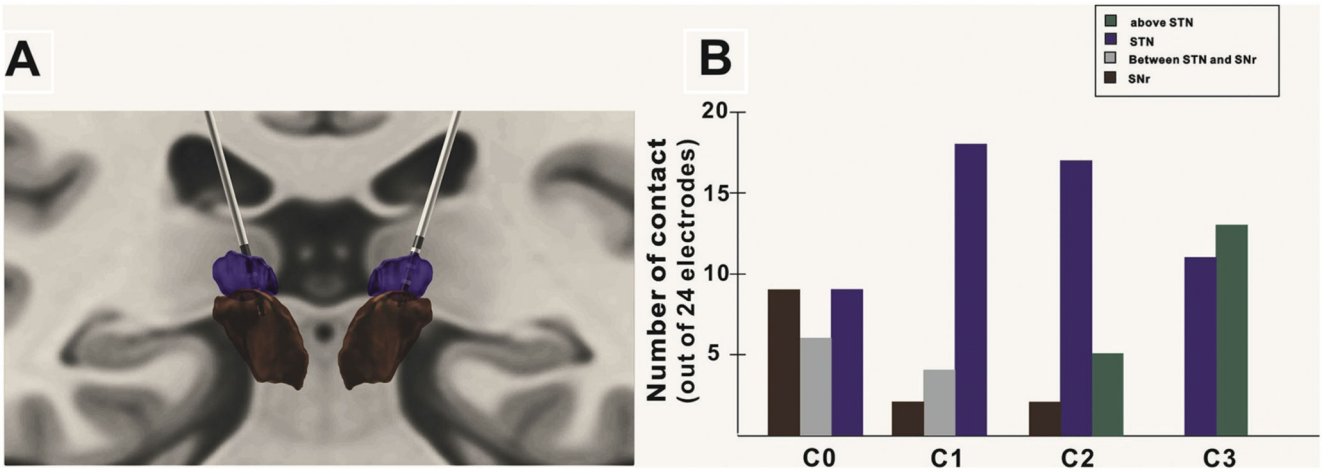

Fig. 1.

Positioning of DBS electrode contacts. (A) STN leads of patient 10 are demonstrated in relation to key structures defined in the Human Motor Thalamus atlas on a coronal MRI section: STN (purple). SNr (brown). (B) Distribution of contacts across the 12 patients in whom MRI reconstruction was possible. (For interpretation of the references to color in this figure legend, the reader is referred to the web version of this article.)

Europe PMC Funders Author Manuscripts

Europe PMC Funders Author Manuscripts

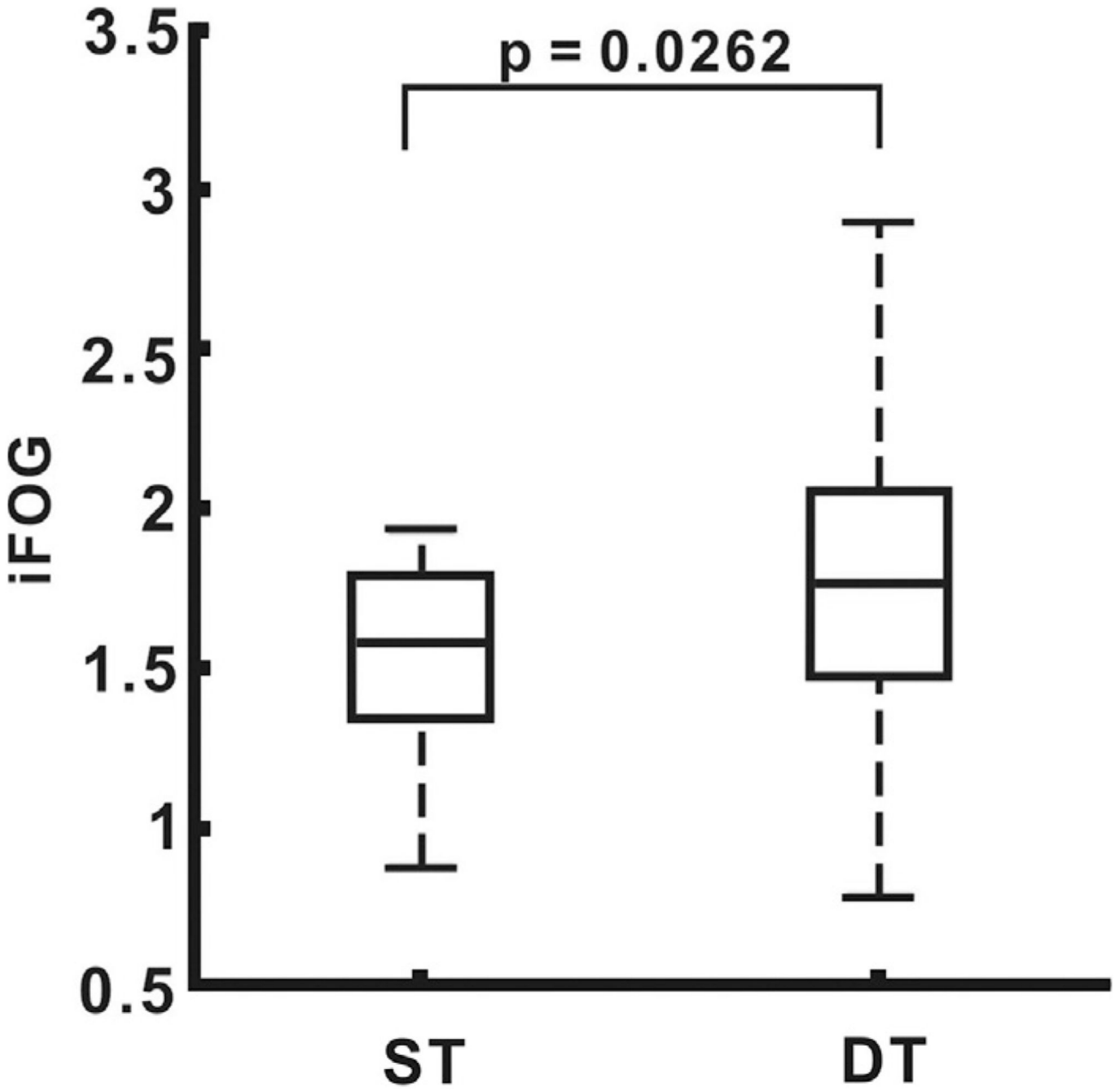

Fig. 2.
Comparison of iFOG between ST and DT.

Europe PMC Funders Author Manuscripts

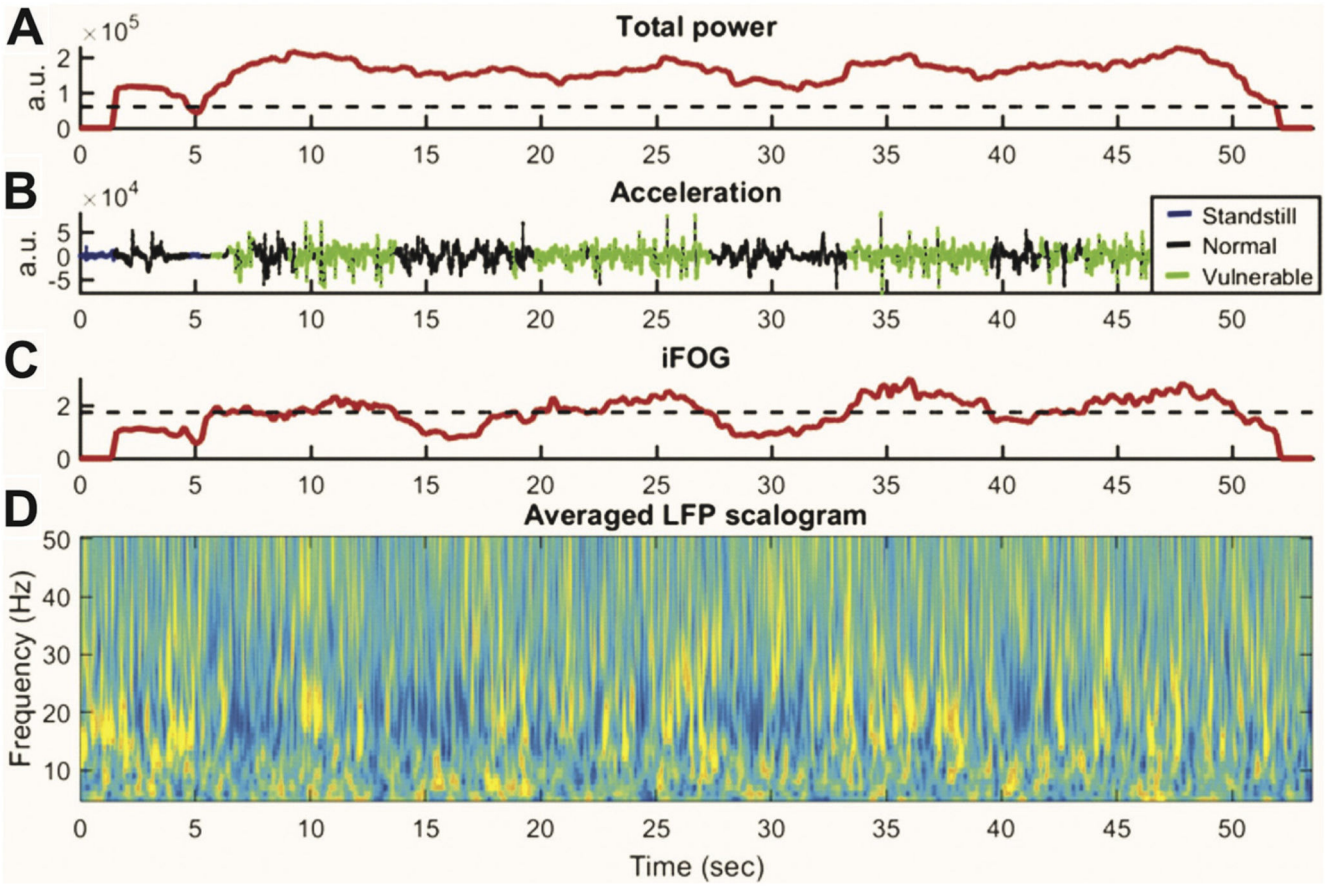

Fig. 3.

Example of simultaneous recordings of ACC recorded by a lumbar accelerometer and STN LFP during gait cycle in patient (case 3). (A) Total power of ACC. Acceleration data were sampled in 3 s windows. (B) Blue indicates standing. Black indicates periods of normal walking. Green indicates the period when gait is vulnerable to freezing, during which the acceleration data show a high-frequency “trembling”. (C) The freezing index, iFOG is calculated from the power in the high frequency band (3–8 Hz) divided by power in the locomotor band (0–3 Hz). The period of vulnerable gait is defined as periods of iFOG exceeding a median threshold. (D) Corresponding averaged LFP across all contact pairs. (For interpretation of the references to color in this figure legend, the reader is referred to the web version of this article.)

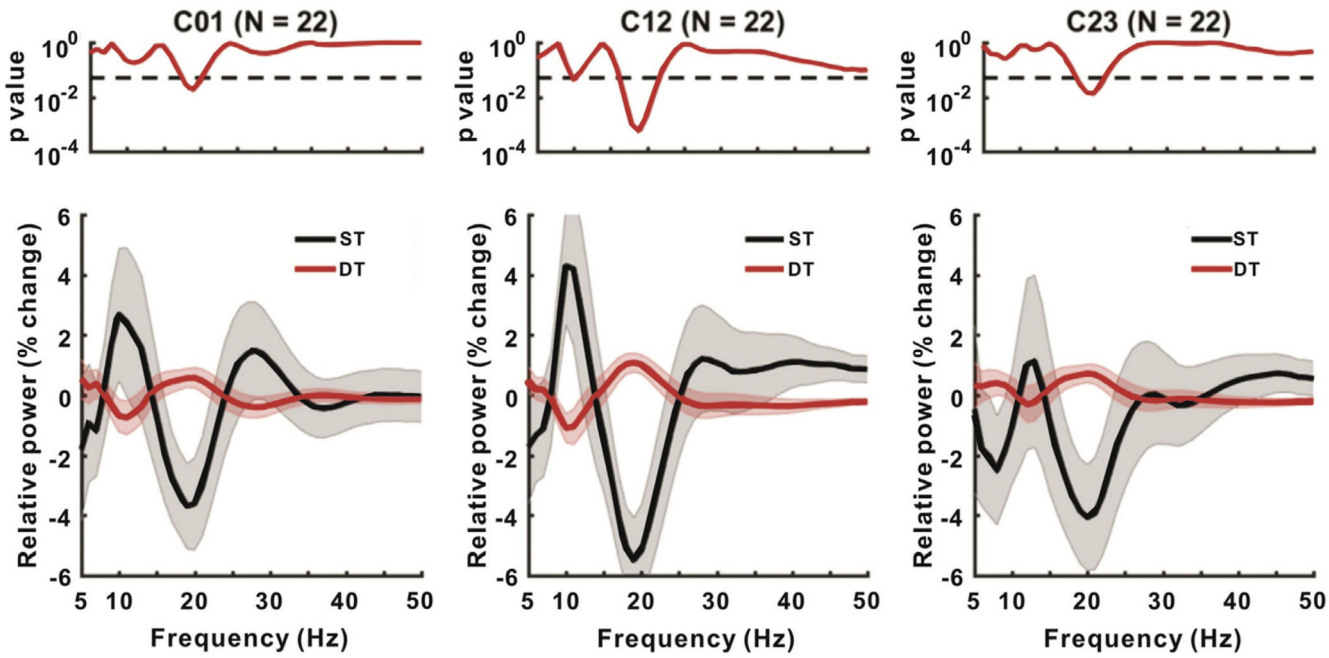

Fig. 4.

Comparison of power change between ST and DT. The upper panels denote the *p*-values for the difference between two conditions at each frequency (serial paired-*t*-test uncorrected for multiple testing, dashing line represents $p = .05$). Lower panels show the relative power in the two conditions in C01, C12 and C23.

Europe PMC Funders Author Manuscripts

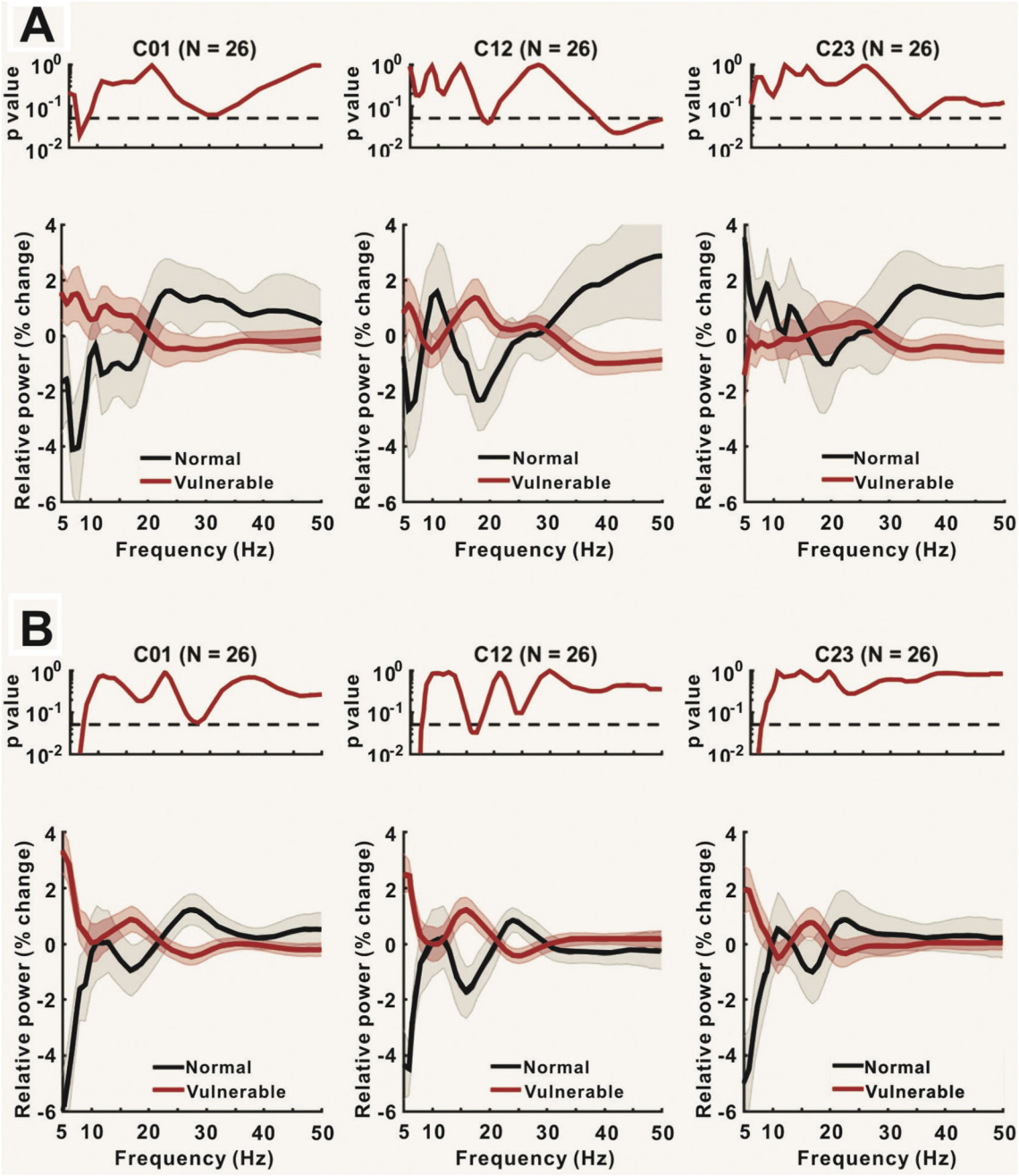

Fig. 5.

Comparison of power change between normal and vulnerable gait periods during ST (A) and DT (B). Upper panels show the p-values for the difference between the two conditions at each frequency. Lower panels show the relative power in the two conditions in C01, C12 and C23.

Europe PMC Funders Author Manuscripts

Table 1

Summary of clinical details.

Case	Age(yr)/Sex	Disease duration (yr)	Pre-op UPDRS Ⅲ On/off Medication	Pre-op UPDRS Ⅱ item 14 On/off	PD phenotype	MMSE	BDI
1	60/F	16	24/45	0/0	PIGD	29	N/A
2	68/M	13	21/32	2/2	PIGD	29	20
3	69/F	20	8/49	0/2	PIGD	30	10
4	52/M	12	20/31	1/3	PIGD	30	11
5	64/M	27	13/28	0/2	PIGD	29	8
6	64/M	10	30/54	0/4	PIGD	30	1
7	64/M	12	7/44	0/0	PIGD	30	7
8	65/F	13	8/30	0/0	PIGD	29	10
9	58/M	9	23/47	0/0	PIGD	29	8
10	63/F	14	19/31	1/1	PIGD	30	11
11	65/F	17	28/49	0/0	PIGD	27	14
12	54/F	16	29/46	1/1	PIGD	30	4
13	64/M	13	22/46	0/1	TD	30	10
14	62/F	21	28/48	2/4	PIGD	30	13
15	55/F	11	19/30	1/3	PIGD	30	17

BDI: Beck Depression Inventory; F: Female; M: Male; MMSE: Mini Mental State Examination; PIGD: Postural instability and gait difficulty; TD: Tremor dominant; UPDRS: Unified Parkinson's disease Rating Scale.

Europe PMC Funders Author Manuscripts

Table 2

Gait performance.

Case	Condition	Velocity, cm/s	Step length, cm (CV, %)	Step time, *sec* (CV, %)	Single support time, sec (CV, %)	Double support time, *sec* (CV, %)
1	ST	N.A.	N. A.	N.A.	N.A.	N.A.
	DT	N.A.	N.A.	N.A.	N.A.	N.A.
2	ST	42.50	30.00 (9.42)	0.66 (2.58)	0.40 (7.46)	0.55 (40.58)
	DT	18.20	11.24 (26.91)	0.52 (19.74)	0.37 (18.31)	0.30 (96.25)
3	ST	62.30	35.21 (14.14)	0.58 (9.97)	0.47 (3.85)	0.32 (3.13)
	DT	84.73	43.87 (14.28)	0.54 (11.36)	0.42 (7.02)	0.32 (31.31)
4	ST	52.85	36.99 (8.38)	0.66 (9.29)	0.53 (11.83)	0.42 (4.61)
	DT	58.20	34.40 (16.52)	0.60 (11.39)	0.43 (8.66)	0.40 (12.96)
5	ST	N.A.	N.A.	N.A.	N.A.	N.A.
	DT	62.80	36.73 (12.31)	0.56 (5.22)	0.32 (9.51)	0.37 (13.69)
6	ST	56.03	39.17 (5.33)	0.76 (4.55)	0.41 (9.07)	0.60 (4.83)
	DT	52.63	36.56 (9.26)	0.69 (9.62)	0.38 (12.37)	0.57 (21.86)
7	ST	77.63	45.63 (6.13)	0.62 (3.68)	0.42 (6.50)	0.35 (7.85)
	DT	63.23	33.68 (12.29)	0.61 (10.61)	0.38 (7.98)	0.39 (7.20)
8	ST	42.90	27.32 (17.63)	0.60 (13.46)	0.34 (17.31)	0.55 (8.32)
	DT	41.48	13.75 (2.66)	0.82 (66.83)	0.40 (43.62)	0.56 (35.61)
9	ST	52.90	32.84 (8.31)	0.69 (4.69)	0.40 (11.88)	0.54 (4.83)
	DT	74.59	35.17 (9.11)	0.55 (8.19)	0.33 (6.57)	0.41 (6.16)
10	ST	41.60	20.51 (13.88)	0.55 (4.69)	0.36 (6.85)	0.41 (5.90)
	DT	40.75	18.85 (17.60)	0.55 (12.47)	0.33 (6.79)	0.41 (9.60)
11	ST	N.A.	N.A.	N.A.	N.A.	N.A.
	DT	N.A.	N.A.	N.A.	N.A.	N.A.
12	ST	88.63	44.86 (6.70)	0.50 (2.78)	0.34 (6.15)	0.31 (6.99)
	DT	63.17	36.94 (9.39)	0.55 (4.29)	0.35 (10.68)	0.40 (11.07)
13	ST	55.30	37.03 (6.79)	0.67 (6.10)	0.48 (5.19)	0.41 (5.88)
	DT	81.10	40.64 (6.43)	0.51 (6.74)	0.38 (3.71)	0.28 (5.75)
14	ST	83.80	41.43 (3.24)	0.52 (2.92)	0.36 (4.62)	0.27 (4.04)
	DT	84.05	40.75 (5.48)	0.50 (3.86)	0.34 (4.31)	0.27 (7.28)
15	ST	N.A.	N.A.	N.A.	N.A.	N.A.
	DT	N.A.	N.A.	N.A.	N.A.	N.A.

Data derived from more affected parkinsonian side.
Data presented as mean (CV, %).
CV = SD/Mean*100%; Coefficient of variation.
N.A. = Not available.
ST = Single-task gait; DT = Dual-task gait.

Europe PMC Funders Author Manuscripts

Table 3

Table contrasting single and dual tasking gaits. Low-beta (15–21 Hz) frequency power was normalized by the average power across both ST and DT. Factors include hemisphere (two levels, left and right), electrode contact (three levels, C01, C12 and C23), and condition (two levels, single and dual task gaits).

Factors	df	SS	MS	F-Value	P-Value
Condition	1	349.89	349.89	14.51	**0.0002**
Contact	2	13.99	6.99	0.29	0.7488
Hemisphere	1	0.36	0.36	0.02	0.9025
Condition*Contact	2	52.49	26.25	1.09	0.3400
Condition*Hemisphere	1	2.91	2.91	0.12	0.7288
Contact*Hemisphere	2	4.74	2.37	0.10	0.9065
Error	122	2941.96	24.11		
Total	131	3366.34			

Significant p values are emboldened.

Europe PMC Funders Author Manuscripts

Table 4

Table for low-beta (15–21 HZ) frequency power in ST normalized by the average power across normal plus vulnerable gait in this condition. Factors include hemisphere (two levels, left and right), electrode contact (three levels, C01, C12 and C23), and condition (two levels, vulnerable and normal gait).

Factors	df	SS	MS	F-Value	*P*-Value
Condition	1	139.26	139.26	4.43	**0.0374**
Contact	2	9.39	4.70	0.15	0.8614
Hemisphere	1	12.35	12.35	0.39	0.5320
Condition*Contact	2	34.63	17.31	0.55	0.5779
Condition*Hemisphere	1	0.11	0.11	0.00	0.9529
Contact*Hemisphere	2	18.81	9.40	0.30	0.7420
Error	122	3835.25	31.44		
Total	131	4049.79			

Significant p values are emboldened.

Europe PMC Funders Author Manuscripts

Table 5

Table of theta (5–8 Hz) frequency power in ST normalized by the averaged power across normal and vulnerable gait in this condition. Factors include hemisphere (two levels, left and right), electrode contact (three levels, C01, C12 and C23), and condition (two levels, vulnerable and normal gait).

Factors	df	SS	MS	F-Value	*P*-Value
Condition	1	128.39	128.39	3.62	0.0596
Contact	2	67.25	33.63	0.95	0.3907
Hemisphere	1	11.05	11.05	0.31	0.5779
Condition*Contact	2	445.60	222.80	6.27	**0.0025**
Condition*Hemisphere	1	0.01	0.01	0.00	0.9865
Contact*Hemisphere	2	9.69	4.84	0.14	0.8726
Error	122	4331.80	35.51		
Total	131	4993.79			

Significant p values are emboldened.

Europe PMC Funders Author Manuscripts

Table 6

Summary for theta (5–8 Hz) frequency power in ST by the averaged power across normal and vulnerable gait, in three different electrode contacts (C01, C12 and C23). Factors include hemisphere (two levels, left and right), and condition (two levels, vulnerable and normal gait).

Contacts	Factors	df	SS	MS	F-Value	P-Value
C01	Condition	1	375.49	375.49	12.96	**0.0009**
	Hemisphere	1	0.32	0.32	0.01	0.9165
	Error	41	1188.00	28.98		
	Total	43	1563.81			
C12	Condition	1	101.72	101.72	2.00	0.1653
	Hemisphere	1	19.88	19.88	0.39	0.5357
	Error	41	2089.79	50.97		
	Total	43	2211.40			
C23	Condition	1	96.78	96.78	3.76	0.0593
	Hemisphere	1	0.54	0.54	0.02	0.8859
	Error	41	1054.02	25.71		
	Total	43	1151.33			

Significant p values are emboldened.

Europe PMC Funders Author Manuscripts

Table 7

Table of low beta (15–21 Hz) frequency power in DT normalized by the averaged power across normal and vulnerable gait in this condition. Factors include hemisphere (two levels, left and right), electrode contact (three levels, C01, C12 and C23), and condition (two levels, vulnerable and normal gait).

Factors	df	SS	MS	F-Value	P-Value
Condition	1	96.10	96.10	10.79	**0.0013**
Contact	2	0.13	0.07	0.01	0.9925
Hemisphere	1	0.42	0.42	0.05	0.8284
Condition*Contact	2	3.06	1.53	0.17	0.8423
Condition*Hemisphere	1	3.84	3.84	0.43	0.5127
Contact*Hemisphere	2	0.53	0.26	0.03	0.9707
Error	122	1086.63	8.91		
Total	131	1190.72			

Significant p values are emboldened.

Europe PMC Funders Author Manuscripts

Table 8

Table of theta (5–8 Hz) frequency power in DT normalized by the averaged power across normal and vulnerable gait in this condition. Factors include hemisphere (two levels, left and right), electrode contact (three levels, C01, C12 and C23), and condition (two levels, vulnerable and normal gait).

Factors	df	SS	MS	F-Value	P-Value
Condition	1	627.79	627.79	40.66	**0.0000**
Contact	2	4.10	2.05	0.13	0.8759
Hemisphere	1	5.11	5.11	0.33	0.5662
Condition*Contact	2	41.92	20.96	1.36	0.2612
Condition*Hemisphere	1	2.77	2.77	0.18	0.6728
Contact*Hemisphere	2	1.84	0.92	0.06	0.9421
Error	122	1883.59	15.44		
Total	131	2567.11			

Significant p values are emboldened.

Europe PMC Funders Author Manuscripts

Table 9

Table showing % Increase in LFP power with elevated FOG vulnerability.

	ST	DT	Paired t-test
Beta (averaged over all contacts)	7.26 ± 8.05%	16.65 ± 7.74%	$p = .3197$
Theta (contact 01)	31.44 ±12.49%	40.37 ± 11.01%	$p = .5469$